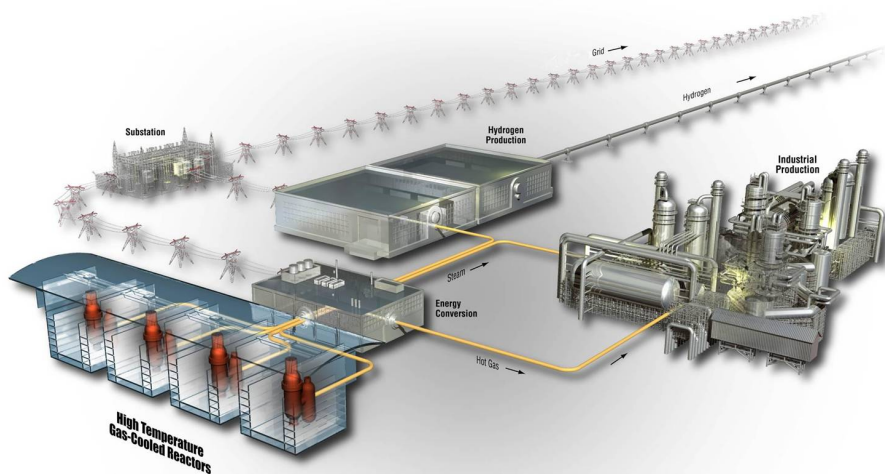


# Particle Image Velocimetry Measurements and Analysis of Bypass Data for a Scaled 6 mm Gap

J. R. Wolf, T. E. Conder, and R. R. Schultz

September 2012

The INL is a  
U.S. Department of Energy  
National Laboratory  
operated by  
Battelle Energy Alliance



#### **DISCLAIMER**

This information was prepared as an account of work sponsored by an agency of the U.S. Government. Neither the U.S. Government nor any agency thereof, nor any of their employees, makes any warranty, expressed or implied, or assumes any legal liability or responsibility for the accuracy, completeness, or usefulness, of any information, apparatus, product, or process disclosed, or represents that its use would not infringe privately owned rights. References herein to any specific commercial product, process, or service by trade name, trade mark, manufacturer, or otherwise, does not necessarily constitute or imply its endorsement, recommendation, or favoring by the U.S. Government or any agency thereof. The views and opinions of authors expressed herein do not necessarily state or reflect those of the U.S. Government or any agency thereof.

# **Particle Image Velocimetry Measurements and Analysis of Bypass Data for a Scaled 6 mm Gap**

**J. R. Wolf, T. E. Conder, and R. R. Schultz**

**September 2012**

**Idaho National Laboratory  
VHTR Program  
Idaho Falls, Idaho 83415**

**<http://www.inl.gov>**

**Prepared for the  
U.S. Department of Energy  
Office of Nuclear Energy  
Under DOE Idaho Operations Office  
Contract DE-AC07-05ID14517**



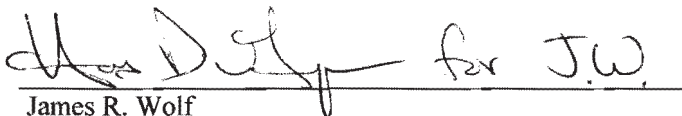
**VHTR TDO Program**

**Particle Image Velocimetry Measurements and  
Analysis of Bypass Data for a Scaled 6 mm Gap**

**INL/EXT-12-26934**

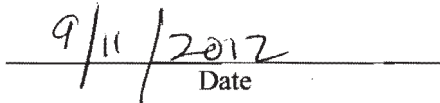
**September 2012**

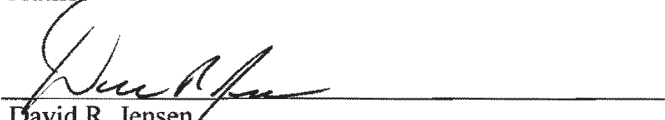
**Approved by:**

 for J.W.

James R. Wolf

Author

 9/11/2012  
Date



David R. Jensen

VHTR QA Lead

 9/11/12  
Date



Diane V. Croson

VHTR TDO Deputy Director

 9/11/12  
Date



## **ABSTRACT**

This report presents the results of fluid dynamics experiments conducted in the matched index-of-refraction flow system at Idaho National Laboratory. The experiments used primarily particle image velocimetry to measure the anticipated bypass flow associated with a prismatic gas turbine-modular helium reactor. A model which represents a stacked junction of six partial fuel blocks with nine coolant tubes and axial and radial gaps was manufactured and installed in the MIR; after which, stereo PIV was employed to measure the flow field within. Measurements were taken in three locations along the length of the model: in the upper plenum and in the midsections of both the large and small fuel blocks. Flow rates were calculated for the coolant channels and gaps for comparison. For the test conditions used, flow in the gaps was determined to be laminar while flow in the coolant channels was transitional. The bypass ratio was estimated to range from 6.8 to 15.8% for the considered flow rates.





## CONTENTS

ABSTRACT.....	v
1. INTRODUCTION.....	1
2. EXPERIMENT CONCEPT.....	1
3. PARTICLE IMAGING VELOCIMETRY.....	4
4. MIR BYPASS PIV MEASUREMENT TECHNIQUE.....	5
5. BYPASS DATA AND ANALYSIS.....	6
6. SUMMARY .....	9
7. REFERENCES .....	10

## FIGURES

Figure 1. Relationship between three prismatic blocks to the “Y” gap geometry of their vertex.....	1
Figure 2. Blow-up of MIR bypass experiment. Plan view.....	2
Figure 3. INL MIR bypass flow experiment assembly. ....	3
Figure 4. Anticipated measurement locations for the INL MIR bypass flow experiment. ....	3
Figure 5. Model outlet showing coolant channels and axial block gaps.....	3
Figure 6. Particle image velocimetry. ....	4
Figure 7. Potential light sheet measurement locations.....	5
Figure 8. Actual gap spacing in the model cross-section.....	6
Figure 9. Locations of data slices.....	6
Figure 10. Actual PIV light sheet locations. ....	7
Figure 11. Typical velocity contour plot ( $Q = 351.15$ L/Min and $x = -1029.5$ mm). ....	7
Figure 12. Typical variation of time averaged velocity in a coolant channel located at $[x, z] = [-1029.5, 103]$ .....	8
Figure 13. Superimposed velocity contour plot ( $Q=351.15$ L/M and $x=1029.49$ mm). ....	9

## TABLES

Table 1. Bypass flow experiment test matrix.....	6
Table 2. Flow Distribution in the bypass model coolant channels and gaps. ....	7
Table 3. Bypass data for a scaled 3 mm gap width.....	9

# Particle Image Velocimetry Measurements and Analysis of Bypass Data for a Scaled 6 mm Gap

## 1. INTRODUCTION

Fluid dynamics experiments are being conducted in the matched-index-of-refraction (MIR) flow system at Idaho National Laboratory (INL) to develop benchmark databases for assessing computational fluid dynamics (CFD) solutions of momentum equations, scalar mixing, and turbulence models for the flow ratios between coolant channels and bypass gaps in the interstitial regions of typical prismatic standard fuel element (SFE) or upper reflector block geometries of typical modular high-temperature gas-cooled reactors (MHTGRs) in the limiting case of negligible buoyancy and constant fluid properties. The experiments use optical techniques, primarily particle image velocimetry (PIV), in the MIR flow system.

## 2. EXPERIMENT CONCEPT

The MIR MHTGR Bypass Flow Experiment will measure flow characteristics in the coolant channels and interstitial gaps between typical prismatic block SFEs or upper reflector blocks.

The configuration of the MIR bypass experiment is scaled to match the bypass geometry for the prismatic core of the MHTGR. Figure 1 shows the relationship of three adjacent prismatic blocks for the MHTGR in the plan view. The interstitial gaps have a maximum width of approximately 3.9 mm prior to irradiation. The gaps between each prismatic block come together at vertices that occur at the corner of three adjacent prismatic blocks (see Figure 1) and form a “Y.” The gaps themselves are characterized by both the gap size (the flow area per unit length) and the frictional pressure drop inherent to the graphite gap walls. In contrast, the vertex passage has, in the limit, a vanishingly small wall influence. Consequently, it is thought that the bypass flow will tend to bias itself to the vertices. Therefore, the interactions between the flow in the gaps and the vertex will be studied in the MIR bypass experiment.

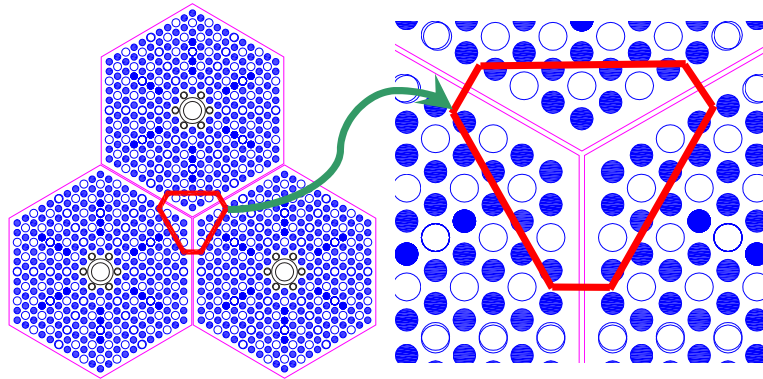


Figure 1. Relationship between three prismatic blocks to the “Y” gap geometry of their vertex.

As described in Schultz 2009,<sup>1</sup> the MIR bypass flow experiment was designed to study the behavior of flow in the gap interstitial region, in particular, to quantify the flow in the gap in relation to the flow in the vertex and the coolant channel regions of SFEs. Because the MIR is an isothermal experiment performed at room temperature, the effects of density gradients and thus the influence of temperature will not be studied. Hence, the MIR experiments will focus on the flow regimes that are momentum dominated as opposed to density-gradient dominated flows.

The experimental concept is shown in the right-hand portion of Figure 1. Typically, the coolant channel Reynolds number based on the channel diameter of the MHTGR at full power is on the order of 50,000 and in excess of 3,500 at low power (~10% power). Design analyses of the planned MIR

experiment indicate that a coolant channel Reynolds number of about 5,700 can be achieved in the planned experiments with the model scaled to 2.016-times the actual size of a SFE to enhance data resolution.

Figure 2 shows a more detailed plan view of the configuration shown in the right-hand side of Figure 1 with the symmetric region of three prismatic blocks that were selected for the MIR bypass experiment. It is important to note that the selected area includes the three coolant channels closest to the vertex of the prismatic SFE and only includes the area of the prismatic SFE that could reasonably be expected to influence flow through the coolant channels and interstitial gaps in this area. Also, the region selected includes the intersection of three prismatic SFEs so that the flow in the area where the three interstitial gaps meet (the vertex) can be studied.

The experimental hardware design shown in Figure 2 includes all three SFE sections that form the interstitial gaps and the gap vertex. The individual SFE sections will be fabricated from fused quartz tubes and solid end caps with holes machined into the end caps. A bypass flow gap of 3 mm width was considered for this set of experiments. However a scaling factor was selected that produced a 6 mm gap in the actual experimental model.

The scaling factor was selected based on the commercially available diameter quartz tubes—used as the coolant channels for the model—that would permit Reynolds numbers comparable to the low power range of an operational prismatic reactor. In addition, careful selection of the scaling factor was important, as it was the key feature to provide adequate spatial resolution for stereo PIV measurements in the coolant channels and gap. Based on this criterion, a tube diameter of 32 mm was chosen.

Figure 3 is an exploded illustration of the model assembly. The assembly includes an aluminum hemispherical dome (red) that models the upper plenum of a typical MHTGR, a quartz inlet plenum (green) that models the region above the upper reflector surface, a quartz model of the coolant channels and interstitial gaps in an SFE (purple and pink), and a model of a second SFE to model the gap between the first vertical SFEs and the next SFE below the upper reflector in the stack.

Figure 4 shows the complete assembly and Figure 5 shows an end view of the model outlet.

Additional information concerning the bypass model design and construction can be found in the NNGP Bypass Control and Measurement Plan.<sup>2</sup>

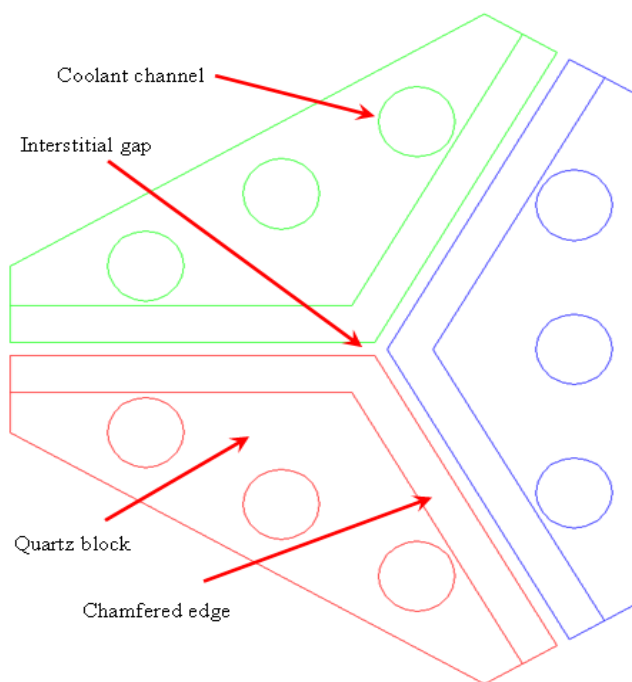


Figure 2. Blow-up of MIR bypass experiment. Plan view.

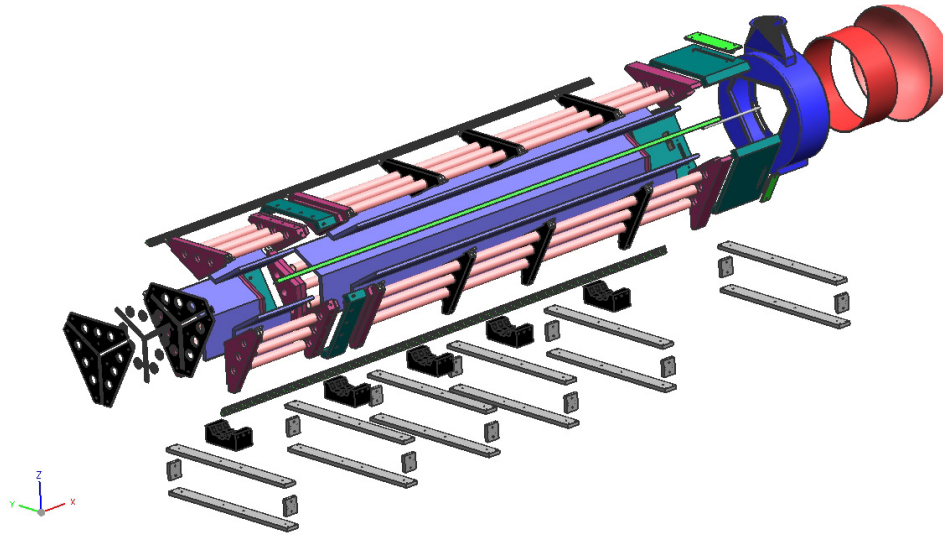


Figure 3. INL MIR bypass flow experiment assembly.

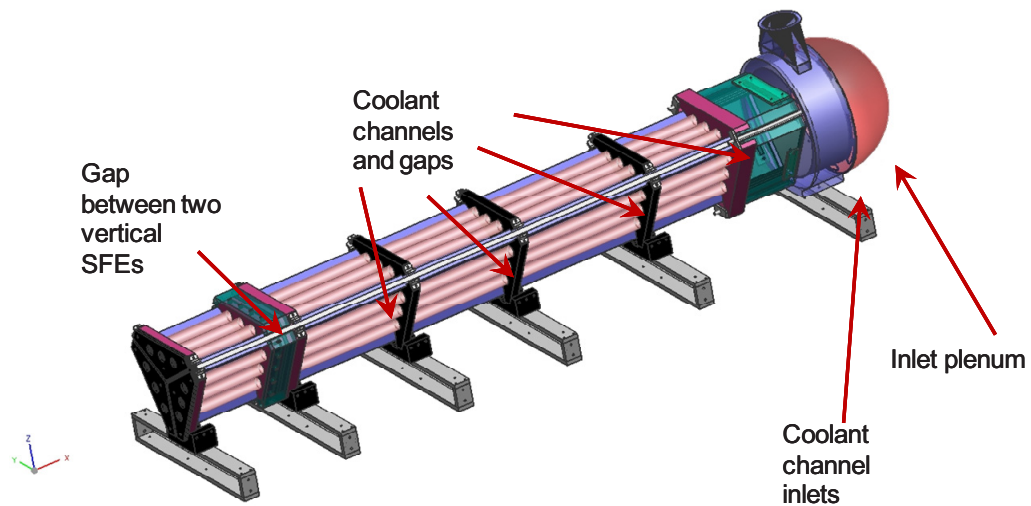


Figure 4. Anticipated measurement locations for the INL MIR bypass flow experiment.

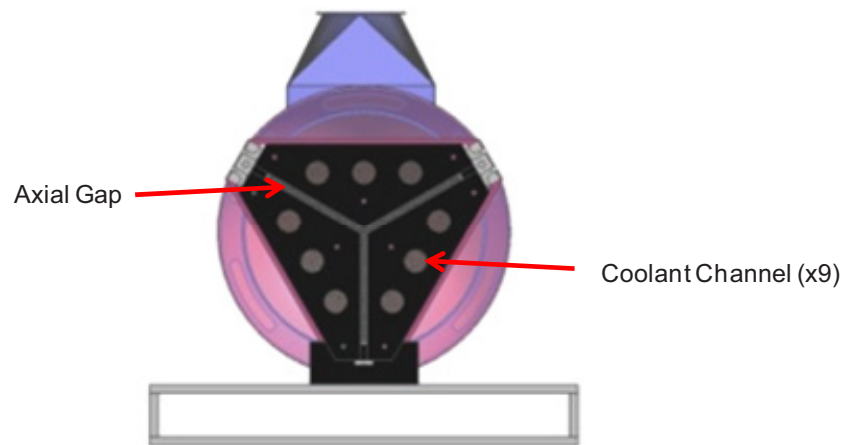


Figure 5. Model outlet showing coolant channels and axial block gaps.

### 3. PARTICLE IMAGING VELOCIMETRY

Most of the measurements used to generate data for CFD validation were provided by the PIV measurements. A flow chart showing the path that PIV advanced instrumentation follows to generate data is shown in Figure 6. In essence, a PIV works by seeding the flow in the experiment with approximately neutrally buoyant particles or at least particles that can be analytically shown to closely follow the fluid streamlines. When a laser pulse is shined on the particles, the resulting reflection shows up as a bright spot on the recorded image, i.e., a digital camera. When a subsequent laser pulse is generated, a comparison between the locations of the images of the same particle over a measured time interval is recorded and provides the distance traveled for a measured time interval. The ratio of these quantities is the velocity in terms of both magnitude and direction. Both two-dimensional and stereo PIVs are used as shown on the left-hand side of Figure 6. With stereo PIVs, such as will be used for the MIR bypass flow experiments, the location of the flowing particles may be tracked in three dimensions. For the MIR bypass flow experiments, the light sheets will be oriented parallel to the axial length of the bypass flow passages as shown in Figure 6. The algorithms (cross-correlation techniques) employed to calculate the velocity vectors are summarized in the upper right side of Figure 6. The data generated by the PIV are shown in the lower right hand side of Figure 6, illustrating a set of vectors that indicate both the magnitude (shown by the length of the vector) and the direction of the particles, and thus the flow in the flow field. Such data will be generated for the MIR bypass flow experiment.

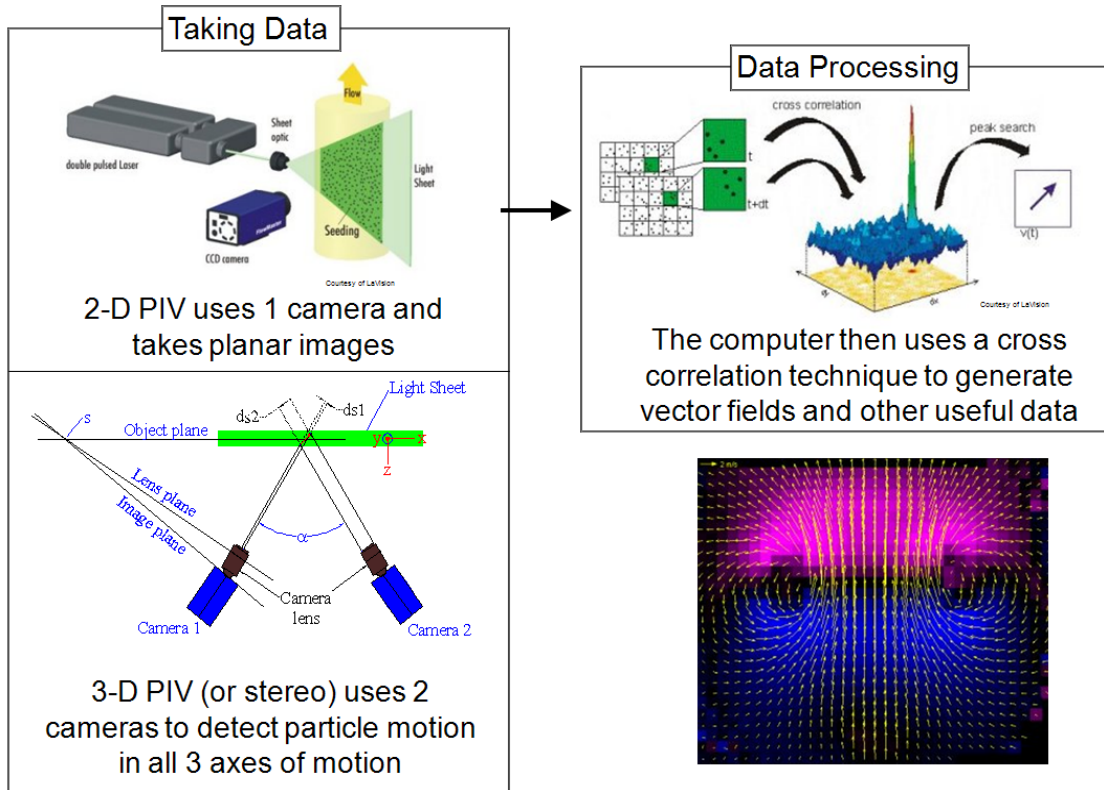


Figure 6. Particle image velocimetry.

Potential light sheet measurement locations are indicated in Figure 7.



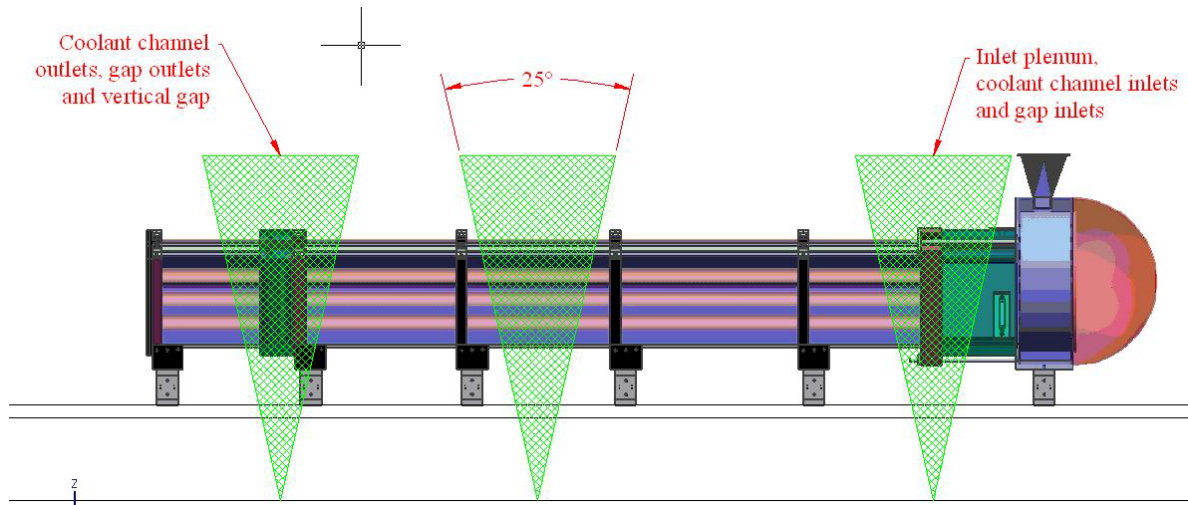


Figure 7. Potential light sheet measurement locations.

#### 4. MIR BYPASS PIV MEASUREMENT TECHNIQUE

Stereo PIV was used to capture the flow field within the upper plenum, coolant channels, and gaps. The flow was seeded with a 12  $\mu\text{m}$  diameter, silver-coated, hollow-glass spheres illuminated in the 532 nm laser light. An Nd:YAG double-pulsed laser projected a light sheet upward through the bottom of the model in the stream-wise direction and two special charge-coupled device cameras continuously imaged the seeding particle movement. Sequential images were broken down into interrogation windows and statistical algorithms were employed to determine particle movement, after which, velocity vectors were calculated over the field of view. A sample size of 500 vector maps were used to ensemble average each flow field measurement.

Measurements were taken in three stream-wise locations: in the upper plenum and in the midsection of both the upper and lower fuel blocks as shown in Figure 7. In these locations, the laser light sheet and cameras were translated across the width of the model, and velocity fields were measured at millimeter intervals—301, 245, and 245 slices were taken in the upper plenum, upper block, and lower block, respectively. As a note, the model's origin was located at the centerline of the model and the inlet of the upper plenum.

During model assembly, spacers were used to achieve uniform axial gaps; however, after installation in the test section the interstitial gap width was measured and found to vary between 5.47 and 7.75 mm. Figure 8 illustrates the actual widths of the interstitial gap for the cross-section of the bypass model measured at the inlet of the upper block. The assembled gap had a cross-sectional area that was approximately 0.0028  $\text{m}^2$ .

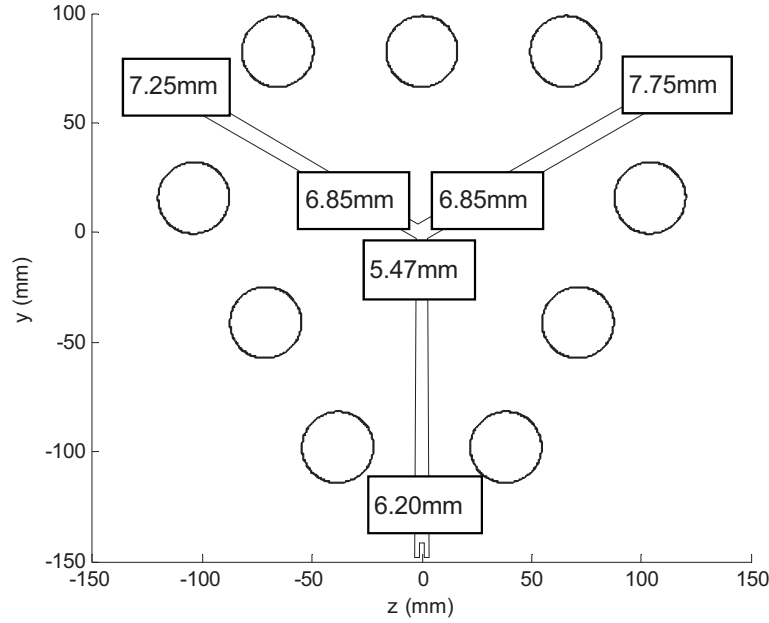


Figure 8. Actual gap spacing in the model cross-section.

## 5. BYPASS DATA AND ANALYSIS

Table 1 is the data collection matrix used for the bypass flow experiment. Inlet conditions were varied to incorporate laminar, transitional, and turbulent flows in the coolant channels, while the axial and radial gaps were held constant at values of 6 and 2 mm, respectively.

Table 1. Bypass flow experiment test matrix.

$Re_{ch}$	Axial Gap (mm)	Radial Gap (mm)	Light Sheet Positions in 1 mm Intervals		
			Upper Plenum (mm)	Upper Block (mm)	Lower Block (mm)
1700	6.05	2.02	$-152 < z < +152$	$-122 < z < +122$	$-122 < z < +122$
3000	6.05	2.02	$-152 < z < +152$	$-122 < z < +122$	$-122 < z < +122$
4800	6.05	2.02	$-152 < z < +152$	$-122 < z < +122$	$-122 < z < +122$

To quantify the flow of the gap in relation to the coolant channels, velocities from the cross-section of the model were needed. To this end, time averaged vector maps at each stream-wise location and flow rate were compiled into matrices, after which, data slices were taken at three locations perpendicular to the flow at  $x = -113.1$ ,  $-1029.5$ , and  $-1928.5$  mm as shown in Figure 9. For the purpose of this paper, the measurements taken in the upper plenum were used solely as a flow rate check.

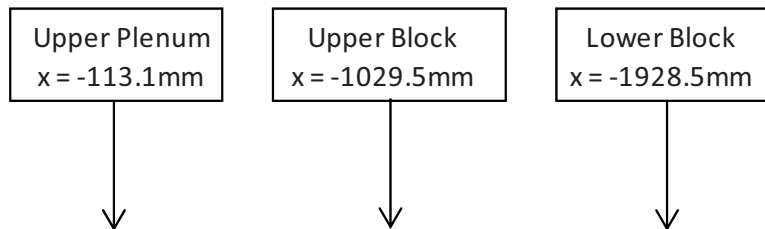


Figure 9. Locations of data slices.

A typical slice of the bypass data located in the upper and lower blocks is displayed in Figure 10. This plot denotes the velocity contours through the cross-section of the model. The PIV cameras had limited optical access to the upper three coolant channels. As such, the PIV algorithms did not detect movement of particles and effectively calculated streaks of zero velocity in these locations.

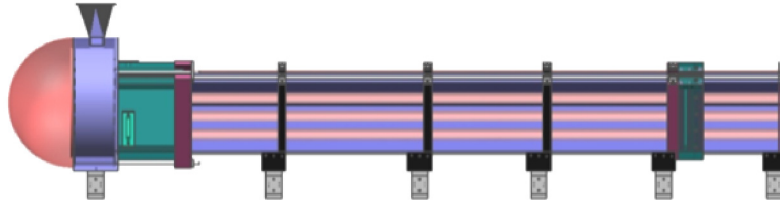


Figure 10. Actual PIV light sheet locations.

A typical slice of the bypass data located in the upper and lower blocks is displayed in Figure 11. This plot denotes the velocity contours through the cross-section of the model. The PIV cameras had limited optical access to the upper three coolant channels. As such, the PIV algorithms did not detect movement of particles and effectively calculated streaks of zero velocity in these locations.

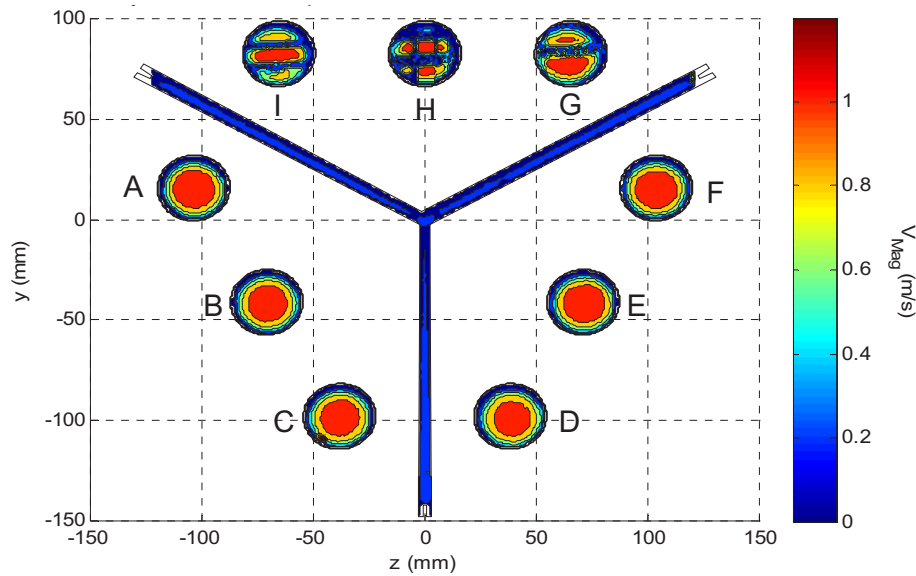


Figure 11. Typical velocity contour plot ( $Q = 351.15 \text{ L/Min}$  and  $x = -1029.5 \text{ mm}$ ).

The distribution of flow through the lower six channels and the gap is presented in Table 2. As expected, the calculated flow rates through the channels were similar for a given inlet condition. It was noted that with an increase in flow rate: the flow through the gap increased, and the variation in flow rate between the coolant channels increased.

Table 2. Flow Distribution in the bypass model coolant channels and gaps.

Total Flow Meter Reading (L/Min)	Stream-wise Location (mm)	Flow Rate (L/Min)						
		A	B	C	D	E	F	Gap
351.1	-1029.5	34.8	34.4	34.7	34.0	35.7	35.5	28.8
579.9		57.6	56.5	57.1	54.0	57.2	57.2	69.5
1004.1		91.0	89.3	90.6	88.1	91.1	91.9	152.7
351.15	-1928.5	35.4	34.6	34.7	35.5	36.6	37.4	24.1



Using the flow rates presented in Table 1, approximate channel Reynolds numbers of 1750, 2800, and 4500 were calculated. Development lengths were predicted for these flows from equations summarized by Munson.<sup>12</sup> It was estimated that fully developed flow would occur near 3.4, 3.0, and 0.6 m for the 351.1, 579.9, and 1004.1 L/Min flow rate cases respectfully. As the model length is 1.91 m, it was understood that only the highest flow case would be fully developed within the coolant channels. Figure 12 shows the typical variation in time-averaged velocity for a flow within a coolant channel. As expected, the lower Reynolds number cases show a developing velocity profile.

Flow rate calculations were computed for each case in the test matrix. It was observed that calculated flow rate error varied between 6.2 and 10.5% when compared to the total flow meter reading. For the lowest and highest flow rates, the bypass flow ratio ranged from 7.3 to 16.94%. Because of the lack of optical access in the upper three tubes of the model, it was assumed these velocity quantities were inaccurate. For this reason, the average velocity of all six lower coolant channels was superimposed on the upper channels to estimate a more realistic flow rate. Figure 13 illustrates the superposition principle using data from Figure 10. In this case, the average flow of channels A, B, C, D, E, and F was superimposed on the upper three channels G, H, and I.

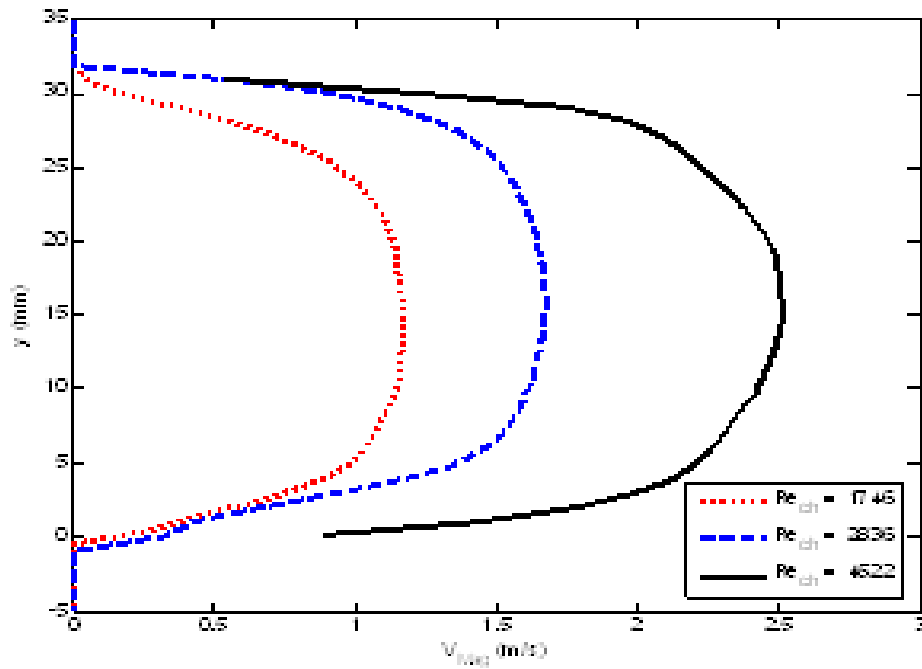


Figure 12. Typical variation of time averaged velocity in a coolant channel located at  $[x, z] = [-1029.5, 103]$ .

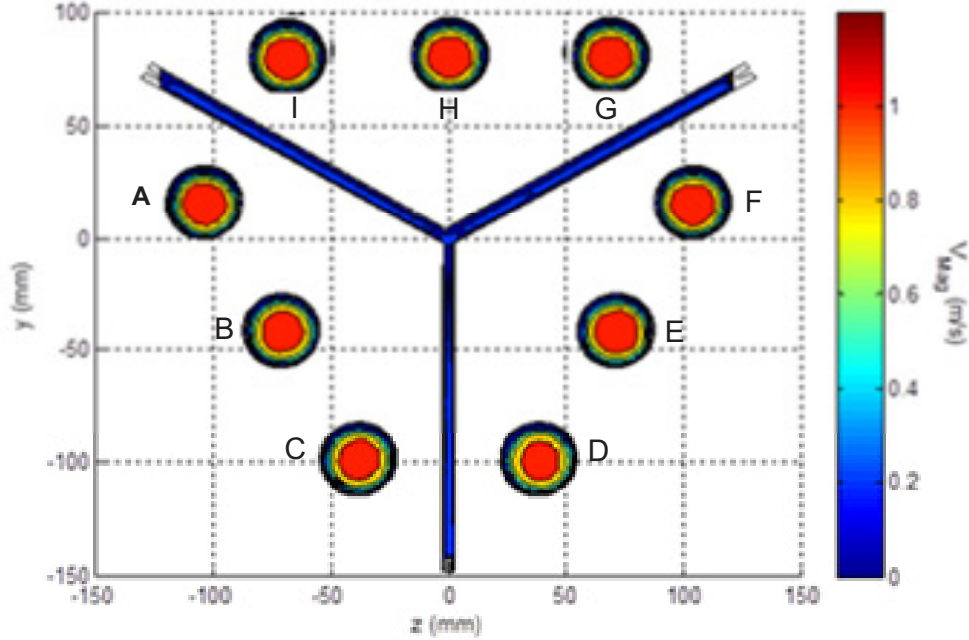


Figure 13. Superimposed velocity contour plot ( $Q=351.15$  L/M and  $x=1029.49$ mm).

Table 3 contains flow rate calculations, errors, and bypass flow ratios considering the superimposed data. As expected, the calculated flow rate error decreased substantially. However, manipulating the data had little effect on the bypass flow ratio. As can be seen from the table, all the gap Reynolds numbers are laminar while the Reynolds number in the coolant channels are turbulent.

Table 3. Bypass data for a scaled 3 mm gap width.

Total Flow Meter Reading (L/Min)	Stream-wise Location (mm)	PIV Calculated Flow Rate (L/Min)	Calculated Flow Rate Error (%)	$Re_{Ch}$	$Re_{Gap}$	Bypass Flow (%)
351.15	-1029.5	342.50	2.46	1746	79	8.40
579.9		579.01	0.015	2836	186	12.00
1004.1		965.55	3.84	4522	413	15.82
351.15	-1928.5	345.46	1.62	1789	66	6.96
579.9		558.94	3.61	2778	150	9.99
1004.1		974.14	2.98	4618	382	14.61

## 6. SUMMARY

Velocity measurements were taken in MIR facility to measure the anticipated bypass flow associated with a prismatic MHTGR. A model which represented a stacked junction of six partial fuel blocks with nine coolant tubes and axial and radial gaps was manufactured and installed in the MIR; after which, stereo PIV was employed to measure the flow field within. Measurements were taken in three locations along the length of the model: in the upper plenum and in the midsection of both the large and small fuel blocks. Flow rates were calculated for the coolant channels and gaps for comparison. For the test conditions used, flow in the gaps was determined to be laminar while flow in the coolant channels was transitional. The bypass ratio was estimated to range from 6.8 to 15.8% for the considered flow rates.

## 7. REFERENCES

1. Schultz, R. R., and M. H. Kim, *Experimental and Analytic Study on the Core Bypass Flow in a Very High Temperature Reactor*, First I-NERI Report, September 2009.
2. Wolf, J. R., “Matched-index-of-refraction MHGTR Prismatic Block Bypass Flow Control and Measurement Plan,” INL PLN-3669, February 7, 2012.